Determine pinhole size

J. M. O. Massey

September 22, 2025

1 Introduction

In the measurement of wall pressure fluctuations in a turbulent boundary layer, we use a microphone cap with a pinhole (PH) to avoid spatial attenuation and aliasing effects. To reconstruct the measured pressure, we must callibrate the treated microphone setup and determine a transfer function (H) that maps PH $\mapsto$ NKD, where NKD is the known pressure measurement. If the PH is too small, the suppression of the signal is too much and H is ill-posed.

Past data has shown that an inner- and outer-scaled part of the premultiplied wall-pressure spectra exist, with the inner-scaled part being invariant to frictional Reynold's number ($\delta^+ \equiv \delta u_\tau/\nu$) (Massey *et al.*, 2025). Figure 1 shows that the peak of the inner-function sits at

$$T^+ \approx 20, \tag{1}$$

where the $\bullet^+$ superscript denotes normalisation by viscous length ν/U_τ. With this region of known behaviour, we can determine the size of the pinhole and correct accordingly.

2 Spatial approximation using Taylor's frozen turbulence hypothesis

Convection velocity can be used to convert temporal fluctuations into spatial structures such that

$$c_x^+ \equiv \frac{\omega^+}{k_x^+} \overset{\substack{\omega^+=2\pi f^+ \\ k_x^+=2\pi/\lambda_x^+}}{\Longleftrightarrow} \frac{c_x^+}{\lambda_x^+} = f^+. \tag{2}$$

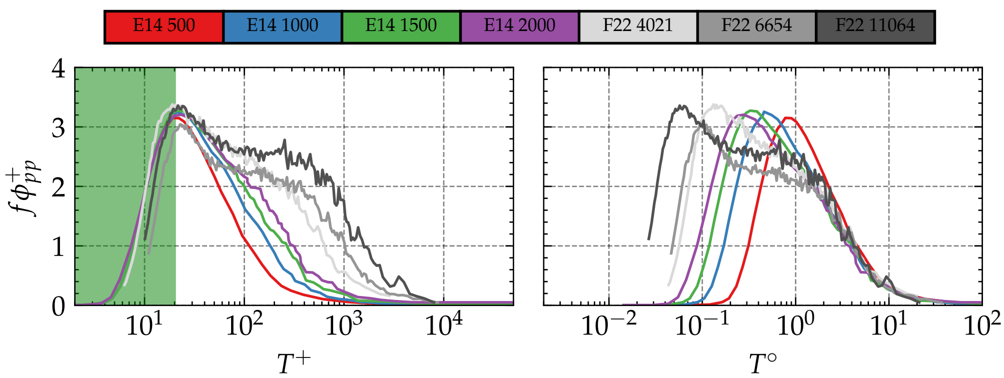

Figure 1: Inner-scaled, pre-multiplied wall-pressure spectra in inner-(**left**) and outer-scaled (**right**) coordinates for a range of Reynolds numbers. The region $T^+ \leq 20$ is highlighted in green. Data from Eitel-Amor *et al.* (2014); Fritsch *et al.* (2020, 2022)

Propagating the equality–acknowledging the relationship $T^+ \equiv 1/f^+$–established in (1) leads to

$$\frac{\lambda_x^+}{c_x^+} < 20 \tag{3}$$

In this context, $\lambda_x^+ \equiv \frac{\ell u_\tau}{\nu}$ is the wavelength of the attenuated structures and c_x^+ is the convection velocity of the structures. The convection velocity of the pressure fluctuations is not constant throughout the boundary-layer (Willmarth & Wooldridge, 1962; Corcos, 1964), but a widely adopted approximation is $c_x^+ \approx 10$ leading to

$$\boxed{\frac{\ell u_\tau}{\nu} < 200.} \tag{4}$$

3 Viscous scales in the Stanford wind tunnel

The plan is to deploy three pinholes, the largest is geared to the atmospheric conditions, the smallest to the highest δ^+, maximum pressure, and one in between. For this study, the boundary-layer thickness is fixed at $\delta = 0.035$ m and the free-stream velocity is fixed at $U_{\mathrm{CL}} = 14$ ms^{-1}.

δ^+	ν/u_τ [μm]	$\ell_{\max}$ [mm]
1500	29.00	5.80
4300	7.97	1.59
8200	4.00	0.80

References

Corcos, G. M. 1964 The structure of the turbulent pressure field in boundary-layer flows. *J. Fluid Mech.* **18** (03), 353.

Eitel-Amor, Georg, Örlü, Ramis & Schlatter, Philipp 2014 Simulation and validation of a spatially evolving turbulent boundary layer up to. *International Journal of Heat and Fluid Flow* **47**, 57–69.

Fritsch, Danny, Vishwanathan, Vidya, Duetsch-Patel, Julie, Gargiulo, Aldo, Lowe, Kevin T. & Devenport, William J. 2020 The Pressure Signature of High Reynolds Number Smooth Wall Turbulent Boundary Layers in Pressure Gradient Family. In *AIAA AVIATION 2020 FORUM*. VIRTUAL EVENT: American Institute of Aeronautics and Astronautics.

Fritsch, Daniel J., Vishwanathan, Vidya, Todd Lowe, K. & Devenport, William J. 2022 Fluctuating Pressure Beneath Smooth Wall Boundary Layers in Nonequilibrium Pressure Gradients. *AIAA Journal* **60** (8), 4725–4743.

Massey, Jonathan M. O., Smits, Alexander J. & McKeon, Beverley J. 2025 Eddy population based model for the wall-pressure spectrum at high Reynolds number. ArXiv:2507.23098 [physics].

Willmarth, W. W. & Wooldridge, C. E. 1962 Measurements of the fluctuating pressure at the wall beneath a thick turbulent boundary layer. *J. Fluid Mech.* **14** (2), 187–210.